JOURNAL OF THEORETICAL AND APPLIED MECHANICS
44, 4, pp. 929-948, Warsaw 2006

DYNAMICS AND CONTROL OF ROTARY CRANES EXECUTING A LOAD PRESCRIBED MOTION

Wojciech Blajer
Krzysztof Kołodziejczyk

Institute of Applied Mechanics, Technical University of Radom
e-mail: w.blajer@pr.radom.pl; kkolodziejczyk@multifox.pl

Manipulating payloads with rotary cranes is challenging due to the underactuated nature of a system in which the number of control inputs/outputs is smaller than the number of degrees-of-freedom. In this paper, the outputs (specified in time load coordinates) lead to servo-constraints on the system. A specific methodology is then developed to solve the arising inverse dynamics problem. Governing equations are derived as a set of index three differential-algebraic equations in state variables and control inputs. An effective numerical code for solving the equations, based on the backward Euler method, is proposed. A feedforward control law obtained this way is then enhanced by a closed-loop control strategy with feedback of actual errors in the load position to provide stable tracking of the required reference load trajectory in presence of perturbations. Some results of numerical simulations are provided.

Key words: rotary cranes, inverse dynamics control, servo-constraints

1. Introduction

Cranes are widely used in transportation and construction. In the industrial practice, they are predominantly operated manually – the operator actuates different joints by joysticks and/or buttons, so that to move the load from its initial position to its desired final destination in the working space along a trajectory, avoiding obstacles and sway. Even though almost the same paths are often repeated, which allows the operator to 'learn' the maneuver, the cycle time is usually relatively large since the operator has to perform the maneuvers slowly in order to avoid inertia-induced excitations, and a considerable percentage of the time is spent on maneuvering the load close to the target point. The latter is usually a trial-and-error process, based on feedback provided by the operator's own vision and assessment, and/or hand signals or

radio communication from a designated assistant at the work zone (Rosenfeld and Shapira, 1998). Automated cranes, after being 'taught' a safe and efficient route between fixed locations of the source and the target, have a potential to play back that route much faster and more accurately than the repeated manual cycles.

High potential of rationalization offered by automatic control systems stimulated an increasing interest and substantial progress in research on modeling and control synthesis of cranes. A good review of the recent developments in the field is provided by Abdel-Rahman *et al.* (2003). Lumped-mass models are most often used, in which the hoisting line is treated as a massless cable, the payload is lumped with a hook and modeled as a point mass, and the cable-hook-payload assembly is modeled as a spherical pendulum, see e.g. Lee (1998) and Ghigliazza and Holmes (2002). Automatic navigation of cranes requires then planning of load motion aimed at minimizing the traveling time under some kinematic limitations such as maximum velocities/accelerations/jerks and/or frequent requirement for vanishing sway during the transfer process and at the target position (Aschemann, 2002).

Cranes belong to a class of underactuated/underconstrained systems, i.e. such controlled mechanical systems in which the number of control inputs/outputs is smaller than the number of degrees of freedom. Control of such systems is a challenging task which has been investigated for a long time (Spong, 1997). In the case of cranes, one of the consequences is that due to the rope flexibility, the undesirable load swing cannot be directly actuated by the available control, and advanced feedback control techniques are needed to suppress the swing and assure precise load positioning (Abdel-Rahman *et al.*, 2003).

In this paper, the problem of dynamics and control of a rotary crane executing a load prescribed motion is viewed from the perspective of constrained motion. The control outputs, expressed in terms of the system states, are treated as servo-constraints on the system (Kirgeov, 1967; Blajer and Kołodziejczyk, 2004; Bajodah *et al.*, 2005). It is noticed, however, that servo-constraints differ from passive constraints in several aspects. Mainly, they are enforced by means of control forces which may have any directions with respect to the manifold of servo-constraints, and in the extreme may be tangent. Such a situation arises in the load trajectory tracking control of rotary cranes, and a specific methodology must be developed to solve the arising 'singular' inverse dynamics problem. After some introductory definitions, a theoretical background for the modeling of the partly specified/actuated motion is given. The initial governing equations arise as index-five Differential-Algebraic Equations (DAEs), and are then transformed to a more tractable index-three form. An effective numerical code for solving the resultant DAEs is used, based on the backward Euler method. A feedforward control law obtained this way is then

enhanced by a closed-loop control strategy with feedback of actual errors in the load position to provide stable tracking of the required reference load trajectory in presence of perturbations. Some results of numerical simulations are provided.

2. Modeling preliminaries

A rotary crane model seen in Fig. 1 is considered. This is a five-degree-of-freedom system, $n = 5$, whose position is described by $\boldsymbol{q} = [\varphi, s, l, \theta_1, \theta_2]^\top$, where φ is the angle of rotation of the girder bridge, s describes the trolley position on the girder, l is the hoisting rope length, and θ_1 and θ_2 are the swing angles seen in the figure. The performance goal is a desired motion of the load, i.e. the control outputs are specified in time by the load coordinates x, y and z in the inertial reference frame XYZ, $\boldsymbol{\gamma}_d(t) = [x_d(t), y_d(t), z_d(t)]^\top$. The control inputs are the torque M_b regulating the bridge rotation angle φ, the force F actuating the trolley position s on the bridge, and the winch torque M_w changing the rope length l, $\boldsymbol{u} = [M_b, F, M_w]^\top$. In this meaning, φ, s and l can be regarded as *controlled coordinates*, while θ_1 and θ_2 can be called *uncontrolled coordinates*.

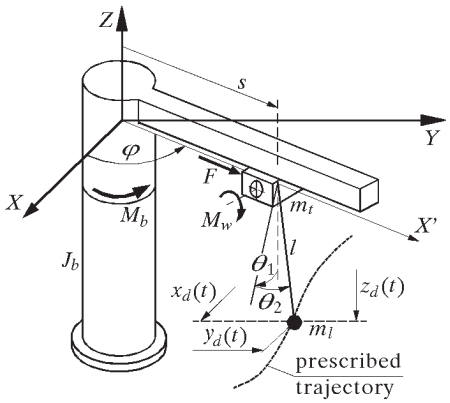

Fig. 1. Rotary crane model

The inverse dynamics control problem considered in this paper is following: *given a prescribed motion of a mechanical system, determine the control inputs that force the system to complete the prescribed motion.* For the case study, the number of control inputs $\boldsymbol{u}$ is equal to the number of outputs $\boldsymbol{\gamma}$, $m = 3$, and it is smaller than the number of degrees of freedom of the system, $m < n$. We deal thus with an *underactuated system in a partly specified motion* (Blajer and Kołodziejczyk, 2004). Prior to developing the solution to the above control

problem, a mathematical model of the crane in the partly specified motion needs to be formulated.

An effective method for derivation of dynamic equations of the crane is the projection method described by Blajer (2001). The starting point are dynamic equations in dependent coordinates $\boldsymbol{p} = [\varphi, x_t, y_t, z_t, \alpha, x, y, z]^\top$, where φ, x, y and z are as defined above, x_t, y_t and z_t are the trolley coordinates in the XYZ frame, and α is the winch rotation angle. Treating initially the bridge, trolley, winch (only its rotation) and load unconstrained from each other, their dynamic equations are simply

$$\begin{aligned} &J_b\ddot{\varphi} = -D_\varphi\dot{\varphi} + M_b && J_w\ddot{\alpha} = -D_\alpha\dot{\alpha} + M_w \\ &m_t\begin{bmatrix}\ddot{x}_t\\ \ddot{y}_t\\ \ddot{z}_t\end{bmatrix} = \begin{bmatrix}-D_s\dot{s}\cos\varphi\\ -D_s\dot{s}\sin\varphi\\ -m_tg\end{bmatrix} + \begin{bmatrix}\cos\varphi\\ \sin\varphi\\ 0\end{bmatrix}F && m\begin{bmatrix}\ddot{x}\\ \ddot{y}\\ \ddot{z}\end{bmatrix} = \begin{bmatrix}0\\ 0\\ -mg\end{bmatrix} \end{aligned} \tag{2.1}$$

where J_b and J_w are the moments of inertia of the bridge and winch relative to their axes of rotation, m_t and m are the trolley and load masses, g is the acceleration of gravity, and D_φ, D_α and D_s are the respective viscous damping coefficients. The initial dynamic equations in $\boldsymbol{p}$ can then be gathered in the following generic matrix form

$$\overline{\mathbf{M}}\ddot{\boldsymbol{p}} = \overline{\boldsymbol{f}} - \overline{\mathbf{B}}^\top\boldsymbol{u} \tag{2.2}$$

where $\overline{\mathbf{M}}$ is the (diagonal) 8×8 generalized mass matrix, $\overline{\boldsymbol{f}}$ is the 8-vector of generalized applied forces, both related to $\boldsymbol{p}$, and $\overline{\mathbf{B}}^\top$ is the 8×3 control matrix ($\overline{\boldsymbol{f}}_c = -\overline{\mathbf{B}}^\top\boldsymbol{u}$ is the 8-vector of generalized control forces related to $\boldsymbol{p}$). Explicit forms of $\overline{\mathbf{M}}$, $\overline{\boldsymbol{f}}$ and $\overline{\mathbf{B}}^\top$ are easy to deduce from equation (2.1).

In order to retrieve the bridge-trolley and winch-load connections, three constraint equations $\overline{\boldsymbol{\Phi}}(\boldsymbol{p}) = \mathbf{0}$ need to be imposed on separated subsystems, i.e.

$$\overline{\boldsymbol{\Phi}} = \begin{bmatrix} -x_t\sin\varphi + y_t\cos\varphi \\ -z_t \\ \sqrt{(x-x_t)^2+(y-y_t)^2+(z-z_t)^2} - l_0 - r_w\alpha \end{bmatrix} = \mathbf{0} \tag{2.3}$$

where l_0 is some initial rope length and r_w is the winch radius. Dynamic equation (2.2) is modified then to the constraint reaction-induced form

$$\overline{\mathbf{M}}\ddot{p} = \overline{\boldsymbol{f}} - \overline{\mathbf{B}}^\top\boldsymbol{u} - \overline{\mathbf{C}}^\top\overline{\boldsymbol{\lambda}} \tag{2.4}$$

where $\overline{\mathbf{C}}(\boldsymbol{p}) = \partial\overline{\boldsymbol{\Phi}}/\partial\boldsymbol{p}$ is the 3×8 constraint matrix

$$\overline{\mathbf{C}} = \begin{bmatrix} C_{11} & -\sin\varphi & \cos\varphi & 0 & 0 & 0 & 0 & 0 \\ 0 & 0 & 0 & -1 & 0 & 0 & 0 & 0 \\ 0 & -\dfrac{x-x_t}{l} & -\dfrac{y-y_t}{l} & -\dfrac{x-z_t}{l} & -r_w & -C_{32} & -C_{33} & -C_{34} \end{bmatrix} \tag{2.5}$$

where

$$C_{11} = -x_t \cos\varphi - y_t \sin\varphi \qquad l = \sqrt{(x-x_t)^2 + (y-y_t)^2 + (z-z_t)^2}$$

The Lagrange multipliers $\overline{\boldsymbol{\lambda}} = [\overline{\lambda}_1, \overline{\lambda}_2, \overline{\lambda}_3]^\top$ stand for the side and vertical reactions between the trolley and bridge and for the tension force in the rope, respectively.

It my be worth noting that the constraint equations given implicitly in equation (2.3) as $\overline{\boldsymbol{\Phi}}(\boldsymbol{p}) = \boldsymbol{0}$ (Schiehlen, 1997; Blajer, 2001) will not in fact be involved in the subsequent formulation of the dynamic equations in $\boldsymbol{q}$, and are needed only if the determination of control reactions $\overline{\boldsymbol{\lambda}}$ is required for any good reason (for evaluation of Coulomb friction effects between the trolley and bridge, for example). Instead, the formulation of dynamic equations in $\boldsymbol{q}$ uses the constraint equations given explicitly. At the position, velocity and acceleration levels these explicit constraint equations are

$$\boldsymbol{p} = \overline{\boldsymbol{g}}(\boldsymbol{q}) \qquad \dot{\boldsymbol{p}} = \overline{\mathbf{D}}(\boldsymbol{q})\dot{\boldsymbol{q}} \qquad \ddot{\boldsymbol{p}} = \overline{\mathbf{D}}(\boldsymbol{q})\ddot{\boldsymbol{q}} + \overline{\boldsymbol{\eta}}(\boldsymbol{q}, \dot{\boldsymbol{q}}) \tag{2.6}$$

where $\overline{\mathbf{D}} = \partial\overline{\boldsymbol{g}}/\partial\boldsymbol{q}$ and $\overline{\boldsymbol{\eta}} = \dot{\overline{\mathbf{D}}}\dot{\boldsymbol{q}}$. In principle, the implicit constraint equations are satisfied identically when expressed in $\boldsymbol{q}$, i.e. $\overline{\boldsymbol{\Phi}}[\overline{\boldsymbol{g}}(\boldsymbol{q})] \equiv \boldsymbol{0}$ and $\dot{\overline{\boldsymbol{\Phi}}} = \overline{\mathbf{C}}\overline{\mathbf{D}}\dot{\boldsymbol{q}} \equiv \boldsymbol{0}$. Since $\dot{\boldsymbol{q}}$ are independent, the latter yields $\overline{\mathbf{C}}\overline{\mathbf{D}} = \mathbf{0} \Leftrightarrow \overline{\mathbf{D}}^\top\overline{\mathbf{C}}^\top = \mathbf{0}$, and $\overline{\mathbf{D}}$ is an orthogonal complement matrix to the constraint matrix $\overline{\mathbf{C}}$; see e.g. Blajer (2001) for more details. For the case at hand, relationship $(2.6)_1$ and the 8×5 matrix $\overline{\mathbf{D}}$ are

$$\begin{bmatrix} \varphi \\ x_t \\ y_t \\ z_t \\ \alpha \\ x_l \\ y_l \\ z_l \end{bmatrix} = \begin{bmatrix} \varphi \\ s\cos\varphi \\ s\sin\varphi \\ 0 \\ (l-l_0)/r_w \\ (s + l\sin\theta_2)\cos\varphi + l\cos\theta_2\sin\theta_1\sin\varphi \\ (s + l\sin\theta_2)\sin\varphi - l\cos\theta_2\sin\theta_1\cos\varphi \\ -l\cos\theta_2\cos\theta_1 \end{bmatrix} \tag{2.7}$$

$$\overline{\mathbf{D}} = \begin{bmatrix} 1 & 0 & 0 & 0 & 0 \\ -s\sin\varphi & \cos\varphi & 0 & 0 & 0 \\ s\cos\varphi & \sin\varphi & 0 & 0 & 0 \\ 0 & 0 & 0 & 0 & 0 \\ 0 & 0 & 1/r_w & 0 & 0 \\ D_{61} & \cos\varphi & D_{63} & D_{64} & D_{65} \\ D_{71} & \sin\varphi & D_{73} & D_{74} & D_{75} \\ 0 & 0 & D_{83} & D_{84} & D_{85} \end{bmatrix}$$

with

$$
\begin{aligned}
D_{61} &= -(s + l\sin\theta_2)\sin\varphi + l\cos\theta_2\sin\theta_1\cos\varphi \\
D_{63} &= \sin\theta_2\cos\varphi + \cos\theta_2\sin\theta_1\sin\varphi \\
D_{64} &= l\cos\theta_2\cos\theta_1\sin\varphi \\
D_{65} &= l\cos\theta_2\cos\varphi - l\sin\theta_2\sin\theta_1\sin\varphi \\
D_{71} &= (s + l\sin\theta_2)\cos\varphi + l\cos\theta_2\sin\theta_1\sin\varphi \\
D_{73} &= \sin\theta_2\sin\varphi - \cos\theta_2\sin\theta_1\cos\varphi \\
D_{74} &= -l\cos\theta_2\cos\theta_1\cos\varphi \\
D_{75} &= l\cos\theta_2\sin\varphi + l\sin\theta_2\sin\theta_1\cos\varphi \\
D_{84} &= l\cos\theta_2\sin\theta_1 \\
D_{85} &= l\sin\theta_2\cos\theta_1
\end{aligned}
$$

Due to complexity of the explicit form of the 8-vector $\overline{\boldsymbol{\eta}}$, it will not be reported here for shortness.

Having explicit constraint equations (2.6) defined, the $n = 5$ dynamic equations of the rotary crane in $\boldsymbol{q}$ are

$$\mathbf{M}(\boldsymbol{q})\ddot{\boldsymbol{q}} + \boldsymbol{d}(\boldsymbol{q}, \dot{\boldsymbol{q}}) = \boldsymbol{f}(\boldsymbol{q}, \dot{\boldsymbol{q}}) - \mathbf{B}^{\top}\boldsymbol{u} \tag{2.8}$$

where $\mathbf{M} = \overline{\mathbf{D}}^{\top}\overline{\mathbf{M}}\overline{\mathbf{D}}$ is the 5×5 generalized mass matrix related to $\boldsymbol{q}$, and $\boldsymbol{d} = \overline{\mathbf{D}}^{\top}\overline{\mathbf{M}}\overline{\boldsymbol{\eta}}$, $\boldsymbol{f} = \overline{\mathbf{D}}^{\top}\overline{\boldsymbol{f}}$ and $\boldsymbol{f}_u = -\mathbf{B}^{\top}\boldsymbol{u}$ (with $\mathbf{B}^{\top} = \overline{\mathbf{D}}^{\top}\overline{\mathbf{B}}$) are the 5-vectors of generalized dynamic, applied and control forces related to $\boldsymbol{q}$. In applications, dynamic equations (2.8) need not to be obtained in an analytical form. Symbolic computer manipulations can be used for its derivation. Here, we will limit ourselves to symbolic form (2.8) of these equations, and demonstrate only the control distribution matrix $\mathbf{B}$ which will be of some use in the sequel

$$\mathbf{B} = \begin{bmatrix} 1 & 0 & 0 & 0 & 0 \\ 0 & 1 & 0 & 0 & 0 \\ 0 & 0 & 1/r_w & 0 & 0 \end{bmatrix} \tag{2.9}$$

It is worth noting that only $\overline{\mathbf{M}}$ and $\overline{\boldsymbol{h}}$ from initial dynamic equations (2.2), and $\overline{\mathbf{D}}$ and $\overline{\boldsymbol{\eta}}$ from explicit constraint equations $(2.6)_{2,3}$ are needed to derive dynamic equations (2.8). The constraint equations in the implicit form $\overline{\boldsymbol{\Phi}}(\boldsymbol{p}) = \mathbf{0}$ and the subsequent constraint matrix $\overline{\mathbf{C}}$ are needed only if the constraint reactions $\overline{\boldsymbol{\lambda}}$ are required. The constraint reactions can be then obtained from (Blajer, 2001)

$$\overline{\boldsymbol{\lambda}}(\boldsymbol{q}, \dot{\boldsymbol{q}}) = (\overline{\mathbf{C}}\overline{\mathbf{M}}^{-1}\overline{\mathbf{C}}^{\top})^{-1}\overline{\mathbf{C}}[\overline{\mathbf{M}}^{-1}(\overline{\boldsymbol{f}} - \overline{\mathbf{B}}^{\top}\boldsymbol{u}) - \overline{\boldsymbol{\eta}}] \tag{2.10}$$

where $\overline{\mathbf{C}}[\boldsymbol{g}(\boldsymbol{q})]$ should be used.

3. Servo-constraint equations

The performance goal of the crane is to execute a desired load trajectory, i.e. $m = 3$ control outputs are time-specified load coordinates

$$\boldsymbol{\gamma}_d(t) = [x_d(t), y_d(t), z_d(t)]^\top$$

The outputs, expressed in terms of the coordinates $\boldsymbol{q}$ as

$$\boldsymbol{c}(\boldsymbol{q}, t) = \boldsymbol{\Phi}(\boldsymbol{q}) - \boldsymbol{\gamma}_d(t) = \boldsymbol{0} \tag{3.1}$$

can be treated as constraints on the system, called *servo-constraints* (Kirgetov, 1967; Bajodah *et al.*, 2005), also called *active, program or control constraints* (Rosen, 1999; Blajer and Kołodziejczyk, 2004) as distinct from *passive (contact) constraints* in the classical sense. After twice differentiating the initial constraint equations with respect to time, the constraint conditions at the acceleration level are

$$\ddot{\boldsymbol{c}} = \mathbf{C}(\boldsymbol{q})\ddot{\boldsymbol{q}} - \boldsymbol{\xi}(\boldsymbol{q}, \dot{\boldsymbol{q}}, t) = \boldsymbol{0} \tag{3.2}$$

where $\mathbf{C} = \partial\boldsymbol{\Phi}/\partial\boldsymbol{q}$ is the 3×5 matrix of the servo-constraints, and $\boldsymbol{\xi} = \ddot{\boldsymbol{\gamma}}_d - \dot{\mathbf{C}}\dot{\boldsymbol{q}}$ is the 3-vector of constraint specified accelerations. For the case at hand, constraint equations (3.1) and the constraint matrix $\mathbf{C}$ defined in equation (3.2) are

$$\boldsymbol{c} = \begin{bmatrix} (s + l\sin\theta_2)\cos\varphi + l\cos\theta_2\sin\theta_1\sin\varphi \\ (s + l\sin\theta_2)\sin\varphi - l\cos\theta_2\sin\theta_1\cos\varphi \\ -l\cos\theta_2\cos\theta_1 \end{bmatrix} - \begin{bmatrix} x_d(t) \\ y_d(t) \\ z_d(t) \end{bmatrix} = \boldsymbol{0}$$

$$\mathbf{C} = \begin{bmatrix} D_{61} & \cos\varphi & D_{63} & D_{64} & D_{65} \\ D_{71} & \sin\varphi & D_{73} & D_{74} & D_{75} \\ 0 & 0 & D_{83} & D_{84} & D_{85} \end{bmatrix} \tag{3.3}$$

where $D_{61}, \ldots, D_{85}$ are as defined in equation (2.7). Analytical expressions for $\boldsymbol{\xi}$ are rather complex and will not be reported here for shortness.

Equation (3.1) is mathematically equivalent to $m = 3$ rheonomic (or time-dependent) holonomic constraints on the system of $n = 5$ degrees of freedom. The resemblance of the load trajectory tracking control problem to the constrained motion case may however be misleading. Assumed $\boldsymbol{c}(\boldsymbol{q}, t) = \boldsymbol{0}$ represents passive constraints, the generalized actuation force $\boldsymbol{f}_u = -\mathbf{B}^\top\boldsymbol{u}$ in dynamic equation (2.8) would be replaced by the generalized constraint reaction force $\boldsymbol{f}_c = -\mathbf{C}^\top\boldsymbol{\lambda}$, where $\mathbf{C}$ is the constraint matrix defined in equation (3.2). While the reactions of ideal passive constraints are by assumption orthogonal to the instantaneous manifold of passive constraints in the configuration

space related to $\boldsymbol{q}$ (Blajer, 2001), the actuating forces may have arbitrary directions with respect to the instantaneous servo-constraint manifold, and in the extreme (some of them) may be tangent. In the latter case, qualitatively, not all of the desired outputs can directly be actuated by the control inputs. A measure of the 'control singularity' is the deficiency in rank of the $m \times m$ matrix $\mathbf{C}\mathbf{M}^{-1}\mathbf{B}^{\top}$, which represents the inner product of the constrained and controlled subspaces in the n-space of crane velocities. For a more detailed discussion on the problem of realization of servo-constraints and the relevant geometrical interpretations, the reader is referred to Blajer and Kołodziejczyk (2004).

In the case at hand, the realization of the three task requirements $\boldsymbol{\gamma}_d(t)$ is enforced by the tension force in the rope, which is the sole attainable control-induced enforcement on the load, $\operatorname{rank}(\mathbf{C}\mathbf{M}^{-1}\mathbf{B}^{\top}) = 1$. Qualitatively, only one task requirement can thus directly (in the orthogonal way) be actuated by the available control, while the realization of two other requirements must be tangent. The value of the tension force can be regulated mainly by M_w, and the direct influence of F and M_b on the tension force is vanishing since of usually small values of θ_1 and θ_2 rope inclination angles. On the other hand, F and M_b can influence the load trajectory realization indirectly by actuating the rope suspension point, which yields appropriate changes in the swing angles θ_1 and θ_2, and causes that the tension force in the rope can change its space orientation and produce required reactions on the load in all three directions. The appropriate changes in θ_1 and θ_2, due to the tangent realization of servo-constraints, can then be viewed as two additional restrictions on the crane configuration, and in this sense the five-degree-of-freedom system is 'fully' specified by three servo-constraints (3.1) and can explicitly be actuated by three control inputs $\boldsymbol{u}$.

4. Governing equations

The initial governing equations of crane motion in the case of the partly specified motion are formed by $n = 5$ kinematic relations $\dot{\boldsymbol{q}} = \boldsymbol{v}$, n dynamic equations (2.8) rearranged with the use of the kinematic relation to $\mathbf{M}(\boldsymbol{q})\dot{\boldsymbol{v}} + \boldsymbol{d}(\boldsymbol{q},\boldsymbol{v}) = \boldsymbol{f}(\boldsymbol{q},\boldsymbol{v}) - \mathbf{B}^{\top}\boldsymbol{u}$, and $m = 3$ servo-constraint equations (3.1), which state together $n + n + m = 5 + 5 + 3 = 13$ Differential-Algebraic Equations (DAEs) in the same number of $2n$ state variables $\boldsymbol{q}$ and $\boldsymbol{v}$, and m control variables $\boldsymbol{u}$. The problem with the DAEs formulated this way is that their *index* is equal to five (Gear and Petzold, 1984; Ascher and Petzold, 1999), which is a measure of singularity/complexity of the DAE system and determines difficulty in numerical treatment. Blajer and Kołodziejczyk (2004)

developed then a scheme for transforming the initial index-five DAEs to an equivalent set of numerically more tractable index-three DAEs, i.e.

$$\begin{aligned}
\dot{\boldsymbol{q}} &= \boldsymbol{v} && & \dot{\boldsymbol{q}} &= \boldsymbol{v} && \text{(4.1a)}\\
\mathbf{D}^{\top}\mathbf{M}\dot{\boldsymbol{v}} &= \mathbf{D}^{\top}(\boldsymbol{f}-\boldsymbol{d}) - \mathbf{D}^{\top}\mathbf{B}^{\top}\boldsymbol{u} && & \mathbf{H}(\boldsymbol{q})\dot{\boldsymbol{v}} &= \boldsymbol{h}(\boldsymbol{q},\dot{\boldsymbol{q}},\boldsymbol{u},t) && \text{(4.1b)}\\
\mathbf{0} &= \mathbf{C}\mathbf{M}^{-1}(\boldsymbol{f}-\boldsymbol{d}) - \mathbf{C}\mathbf{M}^{-1}\mathbf{B}^{\top}\boldsymbol{u} - \boldsymbol{\xi} && \Longleftrightarrow & \mathbf{0} &= \boldsymbol{b}(\boldsymbol{q},\dot{\boldsymbol{q}},\boldsymbol{u},t) && \text{(4.1c)}\\
\mathbf{0} &= \boldsymbol{\Phi}(\boldsymbol{q}) - \boldsymbol{\gamma}_d && & \mathbf{0} &= \boldsymbol{c}(\boldsymbol{q},t) && \text{(4.1d)}
\end{aligned}$$

While equations (4.1a) and (4.1d) are evident, equations (4.1b) and (4.1c) follow from the projection of dynamic equations (2.8) respectively onto complementary unconstrained (unspecified) and constrained (specified) subspaces in the n-space related to $\dot{\boldsymbol{q}}$. The constrained m-subspace is defined by the $m \times n$ (here 3×5) constraint matrix $\mathbf{C}$ introduced in equation (3.2), and the unconstrained k-subspace ($k = n - m$) is defined by the $n \times k$ (here 5×2) matrix $\mathbf{D}$ being an orthogonal complement to $\mathbf{C}$, i.e. $\mathbf{C}\mathbf{D} = \mathbf{0} \Leftrightarrow \mathbf{D}^{\top}\mathbf{C}^{\top} = \mathbf{0}$. The matrix $\mathbf{D}$ satisfying this condition can sometimes be guessed (usually for simple cases only) or determined following a numerically oriented code like the scheme followed from the coordinate partitioning method proposed by Wehage and Haug (1982). Namely, assumed $\mathbf{C}$ is of maximal row-rank, $\operatorname{rank}(\mathbf{C}) = m$, it can always be factorized to $\mathbf{C} = [\boldsymbol{U}, \boldsymbol{W}]$, so that $\mathbf{U}$ and $\mathbf{W}$ are respectively the $m \times k$ and $m \times m$ matrices, and $\det(\mathbf{W}) \neq 0$. The orthogonal complement $\mathbf{D}$ to $\mathbf{C}$ can then be found as

$$\mathbf{D} = \begin{bmatrix} \mathbf{I} \\ -\mathbf{W}^{-1}\mathbf{U} \end{bmatrix} \tag{4.2}$$

where $\mathbf{I}$ is the $k \times k$ (here 2×2) identity matrix.

Projection (4.1b) onto the unconstrained subspace, $\mathbf{D}^{\top}\mathbf{M}\dot{\boldsymbol{v}} + \mathbf{D}^{\top}\boldsymbol{d} = \mathbf{D}^{\top}\boldsymbol{f} - \mathbf{D}^{\top}\mathbf{B}^{\top}\boldsymbol{u}$, states for $k = 2$ differential equations. Projection (4.1c) onto the constrained subspace, $\mathbf{C}\mathbf{M}^{-1}(\boldsymbol{f}-\boldsymbol{d}) - \mathbf{C}\mathbf{M}^{-1}\mathbf{B}^{\top}\boldsymbol{u} - \boldsymbol{\xi} = \mathbf{0}$, represents then $m = 3$ algebraic equations in the system states $\boldsymbol{q}$ and $\boldsymbol{v}$, and control inputs $\boldsymbol{u}$. Due to $\operatorname{rank}(\mathbf{C}\mathbf{M}^{-1}\mathbf{B}^{\top}) = 1$, these three algebraic equations impose only one independent condition on $\boldsymbol{u}$, however, and $k = m - p = 2$ additional restrictions on the crane motion, supplementary to m original requirements (2.10). Therefore, as argued by Blajer and Kolodziejczyk (2004), due to the mixed orthogonal-tangent realization of servo-constraints (2.10), the total number of the original and supplementary motion specifications is $m + k = n = 5$, and thus, in this indirect way, the motion is fully specified.

5. Dynamic analysis and synthesis of control

Similarly to the initial DAEs mentioned in Section 4, governing equations (4.1) represent $n+k+m+m = 5+2+3+3 = 13$ DAEs in the same number of state and control variables $\boldsymbol{q}$, $\boldsymbol{v}$ and $\boldsymbol{u}$, and the index of the DAEs is now equal to three. The solution to DAEs (4.1) are variations in time of state variables for a crane executing a load prescribed motion, $\boldsymbol{q}_d(t)$ and $\boldsymbol{v}_d(t)$, and the control $\boldsymbol{u}_d(t)$ that ensures the realization of this motion.

A simple and effective code for the solution of DAEs (4.1) proposed by Blajer and Kołodziejczyk (2004) uses the Euler backward differentiation approximation method, in which the derivatives $\dot{\boldsymbol{q}}$ and $\dot{\boldsymbol{v}}$ at time $t_{n+1} = t_n + \Delta t$ are approximated by their backward differences, respectively $(\boldsymbol{q}_{n+1} - \boldsymbol{q}_n)/\Delta t$ and $(\boldsymbol{v}_{n+1} - \boldsymbol{v}_n)/\Delta t$, where Δt is the integration time step. Then, given $\boldsymbol{q}_n$ and $\boldsymbol{v}_n$ at time t_n (note that $\boldsymbol{u}_n$ is not involved), the values $\boldsymbol{q}_{n+1}$, $\boldsymbol{v}_{n+1}$ and $\boldsymbol{u}_{n+1}$ at time $t_{n+1} = t_n + \Delta t$ can be found as a solution to the following nonlinear algebraic equations

$$\begin{aligned}
&\frac{\boldsymbol{q}_{n+1} - \boldsymbol{q}_n}{\Delta t} - \boldsymbol{v}_{n+1} = \boldsymbol{0} \\
&\boldsymbol{H}(\boldsymbol{q}_{n+1})\frac{\boldsymbol{v}_{n+1} - \boldsymbol{v}_n}{\Delta t} - \boldsymbol{h}(\boldsymbol{v}_{n+1}, \boldsymbol{q}_{n+1}, \boldsymbol{u}_{n+1}, t_{n+1}) = \boldsymbol{0} \\
&\boldsymbol{b}(\boldsymbol{v}_{n+1}, \boldsymbol{q}_{n+1}, \boldsymbol{u}_{n+1}, t_{n+1}) = \boldsymbol{0} \\
&\boldsymbol{c}(\boldsymbol{q}_{n+1}, t_{n+1}) = \boldsymbol{0}
\end{aligned} \tag{5.1}$$

and in this way the solution can be advanced from time t_n to $t_{n+1} = t_n + \Delta t$.

In order to improve accuracy of the numerical solution, the rough Euler scheme can possibly be replaced by a higher order backward difference approximation method (Gear and Petzold, 1984; Ascher and Petzold, 1999). It may be worth noting however that, becouse the original servo-constraint equations $\boldsymbol{c}(\boldsymbol{q}, t) = \boldsymbol{0}$ are involved in the governing equations, the solution obtained is free from the constraint violation problem, and the truncation errors do not accumulate in time. More strictly, as said before, $m = 3$ algebraic equations $\boldsymbol{b}(\boldsymbol{v}, \boldsymbol{q}, \boldsymbol{u}, t) = \boldsymbol{0}$ impose $p = 1$ independent condition on $\boldsymbol{u}$, and $m - p = 2$ conditions on the crane motion, and in particular on its position $\boldsymbol{q}$. Therefore, the $m + m = 6$ algebraic equations $\boldsymbol{b}(\boldsymbol{v}, \boldsymbol{q}, \boldsymbol{u}, t) = \boldsymbol{0}$ and $\boldsymbol{c}(\boldsymbol{q}, t) = \boldsymbol{0}$ represent $m-p+m = 5$ explicit equations on the five entries of $\boldsymbol{q}$, and the solution $\boldsymbol{q}_d(t)$ is determined only with an accuracy error of solving algebraic equations (5.1). Then, only $\boldsymbol{v}_d(t)$ and $\boldsymbol{u}_d(t)$ are determined with an error followed from the rough backward difference method, which do not accumulate as they are based on the numerically exact solutions $\boldsymbol{q}_d(t)$. The proposed simple code leads thus to reasonable and stable solutions.

The inverse simulation control $\boldsymbol{u}_d(t)$ obtained as a solution to DAEs (4.1) can be used as a feedforward control for a crane executing a prescribed load motion. It should be then enhanced by a feedback control in order to provide stable tracking of the load trajectory in presence of external perturbations and/or modeling inconsistencies. One possibility is to introduce, instead of $\ddot{\boldsymbol{c}} = \boldsymbol{0}$, a stabilized form of the program constraint equations at the acceleration level, $\ddot{\boldsymbol{c}} + \alpha\dot{\boldsymbol{c}} + \beta\boldsymbol{c} + \gamma \int \boldsymbol{c}dt = \boldsymbol{0}$, where α, β and γ are the gain values. Then, after replacing the requirement $\boldsymbol{0} = \boldsymbol{b}(\boldsymbol{q}, \boldsymbol{v}, \boldsymbol{u}, t)$ in equations (4.1c) by its stabilized form

$$\boldsymbol{0} = \mathbf{C}\mathbf{M}^{-1}(\boldsymbol{f} - \boldsymbol{d}) - \mathbf{C}\mathbf{M}^{-1}\mathbf{B}^{\top}\boldsymbol{u} - \boldsymbol{\xi} + \alpha\dot{\boldsymbol{c}} + \beta\boldsymbol{c} + \gamma \int \boldsymbol{c}\, dt = \boldsymbol{b}_{stab}(\boldsymbol{v}, \boldsymbol{q}, \boldsymbol{u}, t) \quad (5.2)$$

a hybrid control can be synthesized from thus modified DAEs (4.1) by using code (5.1). The idea for the crane control with the use of the scheme is shown in Fig. 2.

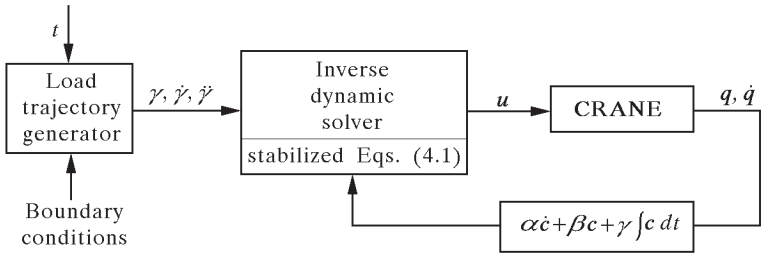

Fig. 2. Hybrid control scheme

6. Numerical simulations

6.1. Load trajectory modeling

During operation, a duty cycle of a crane consists of moving a load from its initial position to its desired final destination in its working space along a trajectory, avoiding obstacles and sway. This requires planning of motion for the given load position. In the present formulation, the load coordinates in the fixed Cartesian frame XYZ (Fig. 1) need to be specified in time, $\boldsymbol{\gamma}_d(t) = [x_d(t), y_d(t), z_d(t)]^{\top}$, where $x_d(t)$, $y_d(t)$ and $z_d(t)$ are appropriately smooth functions of time. A "rest-to-rest" maneuver is usually required (Rosenfeld and Shapira, 1998; Abdel-Rahman *et al.*, 2003), i.e. $\dot{\boldsymbol{\gamma}}_d(t_0) = \dot{\boldsymbol{\gamma}}_d(t_f) = 0$ and $\ddot{\boldsymbol{\gamma}}_d(t_0) = \ddot{\boldsymbol{\gamma}}_d(t_f) = 0$, where t_0 and t_f denote the initial and

final times, respectively. One possibility is to synchronize the outputs using a reference function $s(t)$

$$\boldsymbol{\gamma}_d(t) = \boldsymbol{\gamma}_0 + (\boldsymbol{\gamma}_f - \boldsymbol{\gamma}_0)s(t) \tag{6.1}$$

where $t \in \langle t_0, t_f \rangle$, and $\boldsymbol{\gamma}_0 = [x_0, y_0, z_0]^\top$ and $\boldsymbol{\gamma}_f = [x_f, y_f, z_f]^\top$ are the start and target load positions at the time t_0 and t_f. Having $s(t)$ and its time derivatives, $\dot{\boldsymbol{\gamma}}_d(t)$ and $\ddot{\boldsymbol{\gamma}}_d(t)$ used in the mathematical model can be found as $\dot{\boldsymbol{\gamma}}d(t) = (\boldsymbol{\gamma}_f - \boldsymbol{\gamma}_0)\dot{s}(t)$ and $\ddot{\boldsymbol{\gamma}}_d(t) = (\boldsymbol{\gamma}_f - \boldsymbol{\gamma}_0)\ddot{s}(t)$. For longer traveling distances, the maneuver is often divided into acceleration (I), steady velocity (II) and deceleration (III) phases. The durations of phases I and III are usually determined by some maximum acceleration/jerk limitations, while the duration of phase II may be consequent to the maximum load velocity limitation. Following the idea of Aschemann (2002), the function $s(t)$ used in this paper is

$$\begin{aligned}
s_I(t) &= \frac{1}{\tau - \tau_0}\Big(-\frac{5t^8}{2\tau_0^7} + \frac{10t^7}{\tau_0^6} - \frac{14t^6}{\tau_0^5} + \frac{7t^5}{\tau_0^4}\Big) \\
s_{II}(t) &= \frac{1}{\tau - \tau_0}\Big(t - \frac{\tau_0}{2}\Big) \\
s_{III}(t) &= 1 + \frac{1}{\tau - \tau_0}\Big(\frac{5(\tau - t)^8}{2\tau_0^7} - \frac{10(\tau - t)^7}{\tau_0^6} + \frac{14(\tau - t)^6}{\tau_0^5} - \frac{7(\tau - t)^5}{\tau_0^4}\Big)
\end{aligned} \tag{6.2}$$

where $\tau = t_f - t_0$ and τ_0 is the acceleration/deceleration time. Given $\tau = 20\,\mathrm{s}$ and $\tau_0 = 5\,\mathrm{s}$, reference function (6.2) and their time derivatives are illustrated in Fig. 3.

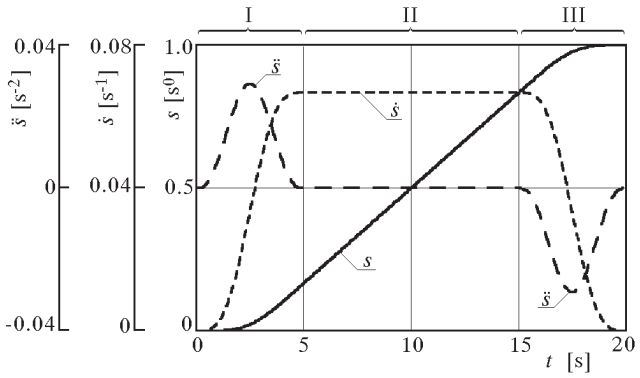

Fig. 3. Reference function and its time-derivatives

Synchronized time functions (6.1) for the reference load coordinates result in a straight line trajectory from the start to target positions. Since the trajectory line cannot cross or pass too close to the tower, for tasks in which

the start and target load positions are at the opposite sides of the tower, the shape function $s(t)$ should rather specify the load cylindrical coordinates, i.e. $\overline{\boldsymbol{\gamma}}_d(t) = \overline{\boldsymbol{\gamma}}_0 + (\overline{\boldsymbol{\gamma}}_f - \overline{\boldsymbol{\gamma}}_0)s(t)$, where $\overline{\boldsymbol{\gamma}} = [r, \phi, z]^\top$, and r and ϕ are the polar coordinates. The required $\boldsymbol{\gamma}_d(t)$, $\dot{\boldsymbol{\gamma}}_d(t)$ and $\ddot{\boldsymbol{\gamma}}_d(t)$ can be then determined following $x_d(t) = r_d(t)\cos\phi_d(t)$ and $y_d(t) = r_d(t)\sin\phi_d(t)$ and the time derivatives of these relations.

6.2. Inverse simulation study

The data used in computations were: $m = 100\,\mathrm{kg}$, $m_t = 10\,\mathrm{kg}$, $J_w = 0.1\,\mathrm{kg\,m^2}$, $r_w = 0.1\,\mathrm{m}$, and $J_b = 480\,\mathrm{kg\,m^2}$. The task requirement was to move the load from the start position to the target position, $\boldsymbol{\gamma}_0 = [5, 0, -5]^\top\,\mathrm{m}$ and $\boldsymbol{\gamma}_f = [-2, 2, -2]^\top\,\mathrm{m}$. Two "rest-to-rest" maneuvers were considered: maneuver 1 along a curvilinear trajectory followed from imposing reference function (6.2) on cylindrical coordinates as described in Section 6.1, and maneuver 2 along a straight line defined in equation (6.1). After applying $\tau = 20\,\mathrm{s}$ and $\tau_0 = 5\,\mathrm{s}$, the obtained reference load trajectories are seen in Fig. 4. Some results of numerical simulations are then reported in Fig. 5, obtained for $\Delta t = 0.01\,\mathrm{s}$ and with no damping in the system ($D_\varphi = D_\alpha = 0$, $D_s = 0$). While the variations of $l(t)$ and $M_w(t)$ are almost the same in the two maneuvers, all the other motion and control characteristics are qualitatively and quantitatively different.

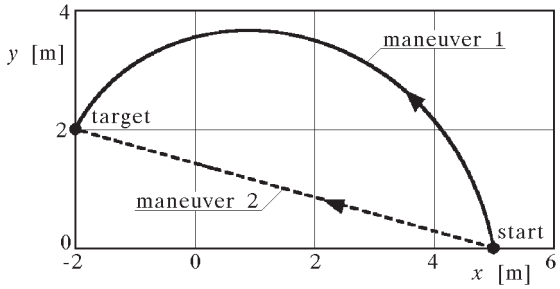

Fig. 4. Maneuvers 1 and 2

6.3. Robustness of hybrid control in perturbed motion

The robustness of the hybrid control described in equation (5.2) and illustrated in Fig. 2 was first tested by applying the inconsistent starting position at t_0 with the load placed 0.5 m above its reference position. Moreover, in the mathematical model used for the direct dynamic simulation, damping related to s and l motions was added, respectively $D_s = 75\,\mathrm{Ns/m}$ and $D_\alpha = 15\,\mathrm{Ns}$, not considered in the model used for the determination of control. The motion disturbed this way was then stabilized along the reference motion by using

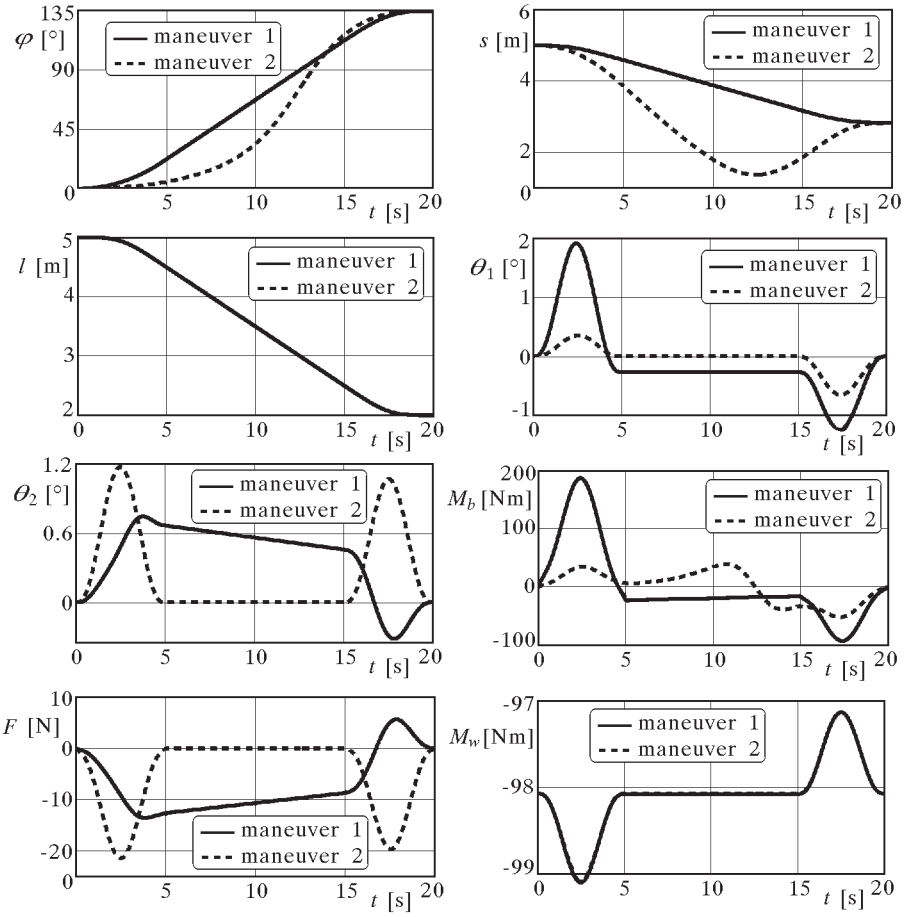

Fig. 5. Crane motion and control in maneuvers 1 and 2

the hybrid control. The gain values used assure the critical damping for a PID scheme (Ostermayer, 1990), i.e. $\alpha^2 = 8\beta$, $32\gamma = \alpha\beta$, and a good choice for β with $\Delta t = 0.01\,\mathrm{s}$ was $\beta = 10$.

Selected simulation results for maneuver 1 as in Section 6.2 are presented in Fig. 6. It can be seen that there is practically no difference in $\varphi(t)$, $s(t)$, $\theta_1(t)$ and $\theta_2(t)$ between the perturbed and reference motions, and the command $M_b(t)$ is not changed either. The initial difference in the vertical load position is quickly damped to the reference values, and this is achieved by an appropriate abrupt change in M_w value at the beginning of simulation. Then, the modeling inconsistency (additional damping in s and l motions) is compensated by appropriate differences in $F(t)$ and $M_w(t)$ relative to the reference control. The differences vanish at the target point when $\dot{s} \to 0$ and $\dot{\alpha} = \dot{l}/r_w \to 0$ (the additional damping vanishes).

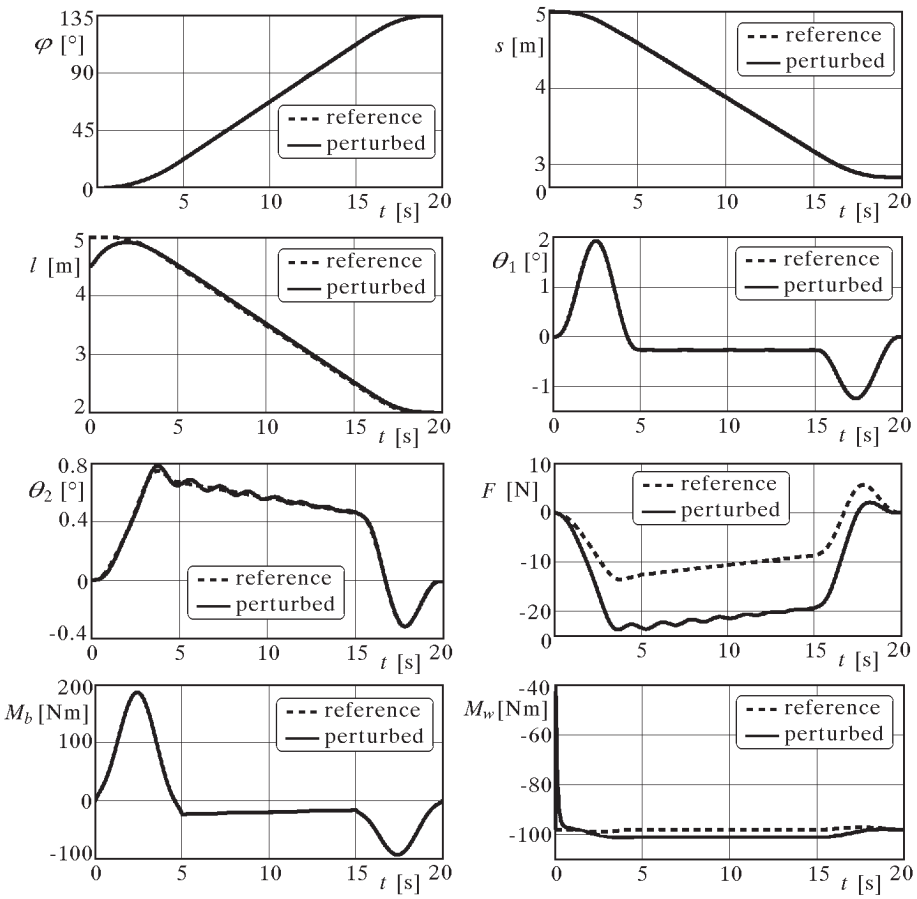

Fig. 6. Simulation of motion in maneuver 1 perturbed by inconsistent initial load position and modeling inconsistencies

As seen from equation (5.2), the feedback control enhanced in the hybrid control is aimed at minimizing the violations of servo-constraints. The initial inconsistency in the load vertical position is thus effectively damped to zero. By contrast, the compensation of the modeling inconsistencies requires some constraint violation to produce additional control commands related to $\alpha\dot{\boldsymbol{c}}+\beta\boldsymbol{c}+\gamma\int \boldsymbol{c}dt$. Both, the damping features and the range of constraint violations required to overcome the modeling inconsistencies are closely related to the values of gain coefficients. In the present experiments, the same gain values for all three outputs were used, and as said $\alpha^2 = 8\beta$ and $32\gamma = \alpha\beta$. In Fig. 7, the effect of different gain values used, obtained for the perturbed motion illustrated in Fig. 6, is seen. The bigger the gain values, the closer is the realization of the perturbed motion to the reference motion. On the other hand, too large gain values lead to instability in simulation, which is a

well-known effect in stabilization of passive constraints as well (Ostermayer, 1990). The gain values limits and/or their optimal values are dependent mainly on the integration time step Δt, and smaller integration time steps allow for bigger gain values. They are also closely related to the system complexity/dimensionality and the type of motion/perturbations simulated. The choice of appropriate gain values is often a trial-and-error process, and disparate gain values for particular outputs are usually involved.

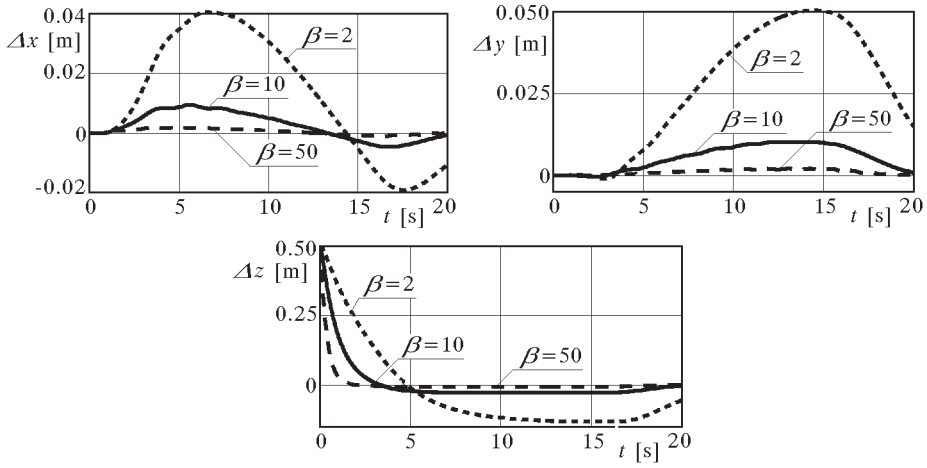

Fig. 7. Differences in load position in perturbed motion for different gain values

The other numerical experiment illustrating the robustness of the hybrid control relates to external perturbations caused by an additional force applied to the load in the negative sense of X direction, not considered in the model used for the determination of control. The force time-profile, which can be regarded as a rough model of wind blow loads on the pay-load, is seen in Fig. 8. The motion disturbed this way was stabilized along the reference motion of maneuver 2 by using the hybrid control. As before, the gain values were $\alpha^2 = 8\beta$, $32\gamma = \alpha\beta$, and $\beta = 30$ was chosen for the integration time step $\Delta t = 0.01$ s.

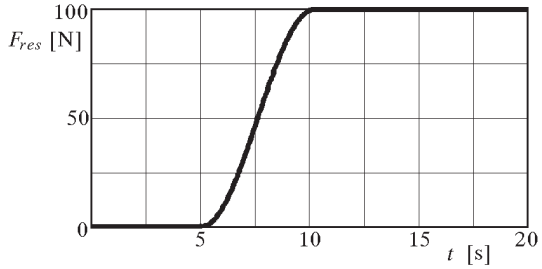

Fig. 8. Profile of perturbation force

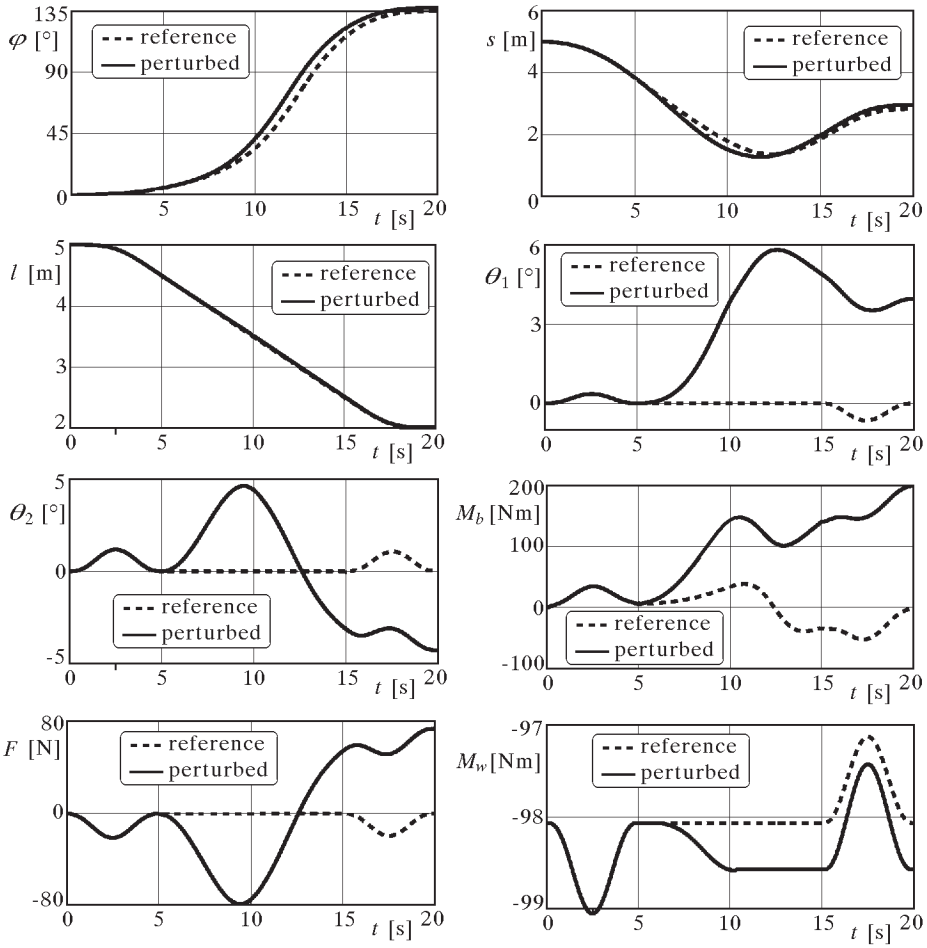

Fig. 9. Simulation of motion in maneuver 2 perturbed by 'wind loads'

The simulation results seen in Fig. 9 show that the 'wind load' F_{res} causes that the rope bends accordingly, and the trolley position and bridge rotation angle differ slightly from the reference values so that to compensate the rope additional bend and to execute the load prescribed motion. The same happens at the target load position. The rope is out of plumb, and the final trolley position and bridge rotation angle differ from their reference values. The 'wind load' effects are compensated by appropriate changes in the control commands which cause that the servo-constraints are realized with a limited accuracy. More strictly, the constraint violations in the Y and Z directions, Δy and Δz, do not exceed ± 0.0004 m during the whole motion, while the violation in the X direction, required to produce the required feedback control commands, is a up to 3.3 cm. This inaccuracy in the load position can be enlarged/diminished by applying smaller/bigger gain values. The effect is illustrated in Fig. 10.

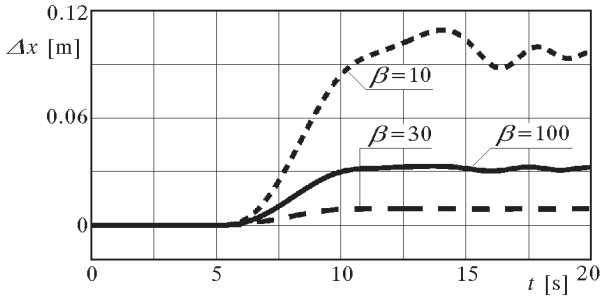

Fig. 10. Difference in the x-position of load in wind-affected motion for different gain values

7. Summary and conclusions

The problem of control of a rotary crane executing a prescribed load trajectory has been viewed from the perspective of constrained system dynamics and inverse dynamics control of an underactuated system. The desired performance goals (specified in time load coordinates), expressed in terms of the system states, lead to servo-constraints on the system. Mixed orthogonal-tangent realization of the servo-constraints by the available crane control is observed, and the tangent realization yields additional conditions on the crane motion. In this sense, the motion of the crane modeled as a five-degree-of-freedom system can be explicitly prescribed by three outputs, and explicitly controlled by available three control inputs.

The governing equations for dynamics and control of a rotary crane executing a load prescribed motion arise as thirteen index-three differential-algebraic equations in the crane state variables and control variables. An effective and stable method for solving the governing DAEs has been proposed and tested through numerical experiments. The solution to the DAEs are motion characteristics of the crane executing the prescribed load trajectory and the control commands (feedforward control) ensuring the prescribed load trajectory realization. The feedforward control law obtained this way was enhanced by a closed-loop control strategy with feedback of the actual errors in the load position.

The reported mathematical model was tested through numerical simulations. The developed computational codes enable one for effective inverse simulation studies related to a wide range of load trajectories/maneuvers. Computational robustness of the developed control strategy in motion perturbed by an inconsistent initial load position, modeling inconsistencies, and external perturbations was proved.

Acknowledgments
The research was supported by grant No. 4 T12C 062$\dot{3}$0.

References

1. ABDEL-RAHMAN E.M., NAYFEH A.H., MASOUD Z.N., 2003, Dynamics and control of cranes: A review, *Journal of Vibration and Control*, **9**, 863-908
2. ASCHEMANN H., 2002, *Optimale Trajektrienplanung sowie modelgestützte Steuerung für einen Brückenkran*, Fortschritt-Berichte VDI, Reihe 8: Mess-, Steuerungs- und Regelungs-technik, Nr. 929, Düsseldorf
3. ASCHER U.M., PETZOLD L.R., 1988, *Computer Methods for Ordinary Differential Equations and Differential-Algebraic Equations*, SIAM, Philadelphia
4. BAJODAH A.H., HODGES D.H., CHEN Y.-H., 2005, Inverse dynamics of servo-constraints based on the generalized inverse, *Nonlinear Dynamics*, **39**, 179-196
5. BLAJER W., 2001, A geometrical interpretation and uniform matrix formulation of multi- body system dynamics, *ZAMM*, **81**, 247-259
6. BLAJER W., KOŁODZIEJCZYK K., 2004, A geometric approach to solving problems of control constraints: theory and a DAE framework, *Multibody System Dynamics*, **11**, 343-364
7. GEAR C.W., PETZOLD L.R., 1984, ODE methods for the solution of differential/algebraic equations, *SIAM Journal of Numerical Analysis*, **21**, 716-728
8. GHIGLIAZZA R.M., HOLMES P., 2002, On the dynamics of cranes, or spherical pendula with moving supports, *International Journal of Non-Linear Mechanics*, **37**, 1211-121
9. KIRGETOV V.I., 1967, The motion of controlled mechanical systems with prescribed constraints (servo-constraints), *PMM*, **21**, 433-466
10. LEE H.-H., 1998, Modeling and control of a three-dimensional overhead crane, *Journal of Dynamic Systems, Measurement, and Control*, **120**, 471-476
11. OSTERMAYER G.-P., 1990, On Baugarte stabilization for differential algebraic equations, In: *Real-Time Integration Methods for Mechanical System Simulation*, Haug E.J. and Deyo R.C. (edit.), NATO ASI Series, Vol. F69, Springer-Verlag, Berlin, 193-207
12. ROSEN A., 1999, Applying the Lagrange method to solve problems of control constraints, *Journal of Applied Mechanics*, **66**, 1013-1015
13. ROSENFELD Y., SHAPIRA A., 1998, Automation of existing tower cranes: economic and technological feasibility, *Automation in Construction*, **7**, 285-298
14. SPONG M.W., 1997, Underactuated mechanical systems, In: *Control Problems in Robotics and Automation*, B. Siciliano and K.P. Valavanis (edit.), Lecture Notes in Control and Information Sciences, Vol. 230, Spinger-Verlag, London

15. Wehage R.A., Haug E.J., 1982, Generalized coordinate partitioning for dimension reduction in analysis of constrained dynamic systems, *Journal of Mechanical Design*, **116**, 1058-1064

Dybanika i sterowanie żurawiem wieżowym realizującym zadany ruch ładunku

Streszczenie

Manewrowanie ruchem ładunku przez żurawie wieżowe jest zadaniem trudnym między innymi ze względu na fakt, że liczba kanałów sterowania (równa liczbie regulowanych współrzędnych ładunku) jest mniejsza od liczby stopni swobody żurawia. W pracy zadane w czasie współrzędne ładunku prowadzą do sformułowania serwowięzów (więzów programowych) nakładanych na ruch układu. Prezentowana jest następnie metoda rozwiązania tego szczególnego zadania symulacji dynamicznej odwrotnej jako zadania ruchu programowego niezupełnego. Równania ruchu programowego formułowane są w postaci układu równań różniczkowo-algebraicznych o indeksie trzy, względem zmiennych stanu i parametrów sterowania żurawiem. Proponowania jest prosta i skuteczna metoda numerycznego całkowania tych równań, wykorzystująca schemat Eulera różnic skończonych wstecznych. Otrzymywane tą drogą sterowanie nominalne uzupełniane jest następnie sterowaniem w układzie zamkniętym zapewniającym stabilną realizację programowego ruchu ładunku w warunkach ruchu zaburzonego i nieścisłości modelowania matematycznego. Prezentowane są wybrane wyniki numerycznej symulacji ruchu i sterowania żurawiem realizującym zadany ruch ładunku.

Manuscript received May 19, 2006; accepted for print July 10, 2006